

Jana TURJANICOVÁ\*, Eduard ROHAN\*\*, Salah NAILI\*\*\*, Robert CIMRMAN†\*\*\*\*

MODELLING OF CORTICAL BONE TISSUE AS A FLUID SATURATED DOUBLE-POROUS  
MATERIAL - PARAMETRIC STUDY

MODELOVÁNÍ TKÁŇE KORTIKÁLNÍ KOSTI JAKO TEKUTINOU PROSYCENÝ MATERIÁL S  
DVOJÍ POROZITOU - PARAMETRICKÁ STUDIE

**Abstract** In this paper, the cortical bone tissue is considered as a poroelastic material with periodic structure represented at microscopic and mesoscopic levels. The pores of microscopic scale are connected with the pores of mesoscopic scale creating one system of connected network filled with compressible fluid. The method of asymptotic homogenization is applied to upscale the microscopic model of the fluid-solid interaction under a static loading. Obtained homogenized coefficients describe material properties of the poroelastic matrix fractured by fluid-filled pores whose geometry is described at the mesoscopic level. The second-level upscaling provides homogenized poroelastic coefficients relevant on the macroscopic scale. Furthermore, we study the dependence of these coefficients on geometrical parameters on related microscopic and macroscopic scales.

**Abstrakt** Tento článek představuje model tkáně kortikální kosti jako materiálu s periodickou strukturou reprezentovanou na mikroskopické a mezoskopické úrovni. Póry na těchto dvou úrovních jsou vzájemně propojené a vytvářejí tak souvislý objem vyplněný stlačitelnou tekutinou. Aplikací metody asymptotické homogenizace na mikroskopický problém interakce mezi tekutinou a elastickým skeletem jsou získány homogenizované koeficienty popisující materiálové vlastnosti poroelastické matrice nasycené tekutinou. Na mezoskopické úrovni je tato matrice perforována systémem kanálů této vyšší úrovně. Další aplikací metody homogenizace na této úrovni jsou získány efektivní poroelastické koeficienty popisující chování materiálu na makroskopické úrovni. Dále je provedena studie závislosti těchto koeficientů na geometrických parametrech vztahujících se k mikroskopické a makroskopické úrovni.

**Keywords** Poroelasticity, homogenization, porous medium, osteon, cortical bone, tissue modelling, unfolding method.

## 1 INTRODUCTION

The cortical bone can be represented as hierarchical material with several scales of structure. At the level, bone tissue is formed as a porous structure incorporating collagen molecules and mineral crystals. However, this study is oriented on the microstructural level of the bone, specifically to a single bone osteon. At the macroscopic level the bone is formed by osteons.

The osteon is a hollow structure of approximately cylindrical shape; in the cortical bone of

---

\* Bc., Department of Mechanics, Faculty of Applied Sciences, University of West Bohemia, Univerzitní 8, Plzeň, tel. (+420) 377 632 301, e-mail: turjani@students.zcu.cz

\*\* Prof. Dr. Ing. DSc., Dept. of Mechanics, New Technologies for Information Society – the Center of Excellence, Univerzitní 8, Plzeň, tel. (+420) 377 632 311, e-mail: rohan@kme.zcu.cz

\*\*\* Prof., Laboratoire modélisation et simulation multi échelle, Université Paris-est, 61 avenue du Général de Gaulle, Créteil cedex, France, e-mail: salah.naili@univ-paris-est.fr

\*\*\*\* Ing. Ph.D., New Technologies Research Centre, University of West Bohemia in Pilsen, Univerzitní 8, Plzeň, e-mail: cimrman3@ntc.zcu.cz

humans and some other species, its radius ranges  $100 \div 150\mu\text{m}$ . The hollow space in the center of the osteon (the diameter about  $10 \div 15\mu\text{m}$  is called the Haversian canal, which usually contains blood vessels, nerves and bone fluid which penetrate into secondary porosities distributed in the wall of osteons. These are formed by small tunnels ( $\approx 0.5 \div 2\mu\text{m}$ ) called canaliculi, connecting the Haversian canal with lacunae. This level can be called canalicular porosity level.

The lacunae are shaped in the forms of ellipsoids, each containing one osteocyte. The principal axes of lacunae are approximately  $25 \times 10 \times 5\mu\text{m}$ , [4]. The network consisting of lacunae mutually connected by canaliculi is called lacunar-canalicular porosity level.

Because of the large number of lacunae and canaliculi in each osteon, a direct modelling of such a complex structure would lead to prohibitively complex problems even if merely a static loading was considered. Therefore, a model based on two-level homogenization with a periodic structure ansatz applied at each level was proposed, to obtain material properties of the bone osteon matrix.

We consider the following two levels of homogenization.

- $\alpha$ -level - upscaling from the canalicular porosity level to obtain the material model describing effective behaviour relevant at the  $\beta$ -level of heterogeneity. The bone matrix is constituted by a solid perforated by canaliculi.
- $\beta$ -level - upscaling from the lacunar-canalicular porosity level to obtain the material model describing effective behaviour at the level of osteones. The heterogeneous structure is formed by the poroelastic matrix with connected porosity (the canaliculi) drained in the ellipsoidal fractures representing lacunae.

## 2 MATHEMATICAL MODEL

In this section we record results of the two-level homogenized model proposed in [3].

### 2.1 Homogenization of the $\alpha$ -level

Domain  $\Omega^\alpha \subset \mathbb{R}^3$  is decomposed into the (solid) matrix  $\Omega_m^{\alpha,\varepsilon}$  and canals  $\Omega_c^{\alpha,\varepsilon}$  as follows:

$$\Omega^\alpha = \Omega_m^{\alpha,\varepsilon} \cup \Omega_c^{\alpha,\varepsilon} \cup \Gamma^{\alpha,\varepsilon}, \quad \Omega_c^{\alpha,\varepsilon} = \Omega^\alpha \setminus \Omega_m^{\alpha,\varepsilon}, \quad \Gamma^{\alpha,\varepsilon} = \Omega_m^{\alpha,\varepsilon} \cap \Omega_c^{\alpha,\varepsilon}. \quad (1)$$

Above and throughout the text, by  $\varepsilon$  we refer to the scale parameter, the ration between two characteristic lengths associated with the micro- and meso-scales.

If the static loading is assumed, the deformation of the fluid-solid interaction is governed by the following problem: Find a displacement field  $\mathbf{u}^{\alpha,\varepsilon}$  and a fluid pressure  $\bar{p}^{\alpha,\varepsilon}$  such that

$$-\nabla \cdot (\mathbb{D}^{\alpha,\varepsilon} \nabla^S \mathbf{u}^{\alpha,\varepsilon}) = \mathbf{f}^{\alpha,\varepsilon}, \quad \text{in } \Omega_m^{\alpha,\varepsilon} \quad (2)$$

$$\mathbf{n}^m \cdot \mathbb{D}^{\alpha,\varepsilon} \nabla^S \mathbf{u}^{\alpha,\varepsilon} = \mathbf{g}^{\alpha,\varepsilon}, \quad \text{on } \partial_{ext} \Omega_m^{\alpha,\varepsilon} \quad (3)$$

$$\mathbf{n}^m \cdot \mathbb{D}^{\alpha,\varepsilon} \nabla^S \mathbf{u}^{\alpha,\varepsilon} = -\bar{p}^{\alpha,\varepsilon}, \quad \text{on } \Gamma^{\alpha,\varepsilon}. \quad (4)$$

and (by  $\tilde{\cdot}$  we denote a matrix-to-canal extension)

$$\int_{\partial \Omega_c^{\alpha,\varepsilon}} \tilde{\mathbf{u}}^{\alpha,\varepsilon} \cdot \mathbf{n}^c dS_x + \gamma^\alpha \bar{p}^{\alpha,\varepsilon} |\Omega_c^{\alpha,\varepsilon}| = -J^{\alpha,\varepsilon}, \quad (5)$$

where  $\mathbb{D}^{\alpha,\varepsilon}$  is the elasticity fourth-order tensor of the matrix,  $\gamma^\alpha$  is the fluid compressibility and  $\mathbf{g}^{\alpha,\varepsilon}$  and  $\mathbf{f}^{\alpha,\varepsilon}$  are applied surface-force and volume-force fields. Below we describe the homogenized model of poroelasticity consisting of local problems for so-called corrector basis functions which are involved in expressions of the homogenized coefficients.

## 2.2 Homogenized problem on $\alpha$ -level

The periodic microstructure is generated by the reference periodic cell (RPC)  $Y^\alpha$  decomposed into the matrix part  $Y_m^\alpha$  and canals  $Y_c^\alpha$ , as follows:

$$Y^\alpha = Y_m^\alpha \cup Y_c^\alpha \cup \Gamma_Y^\alpha, \quad Y_c^\alpha = Y^\alpha \setminus \bar{Y}_m^\alpha, \quad \Gamma_Y^\alpha = \bar{Y}_m^\alpha \cap \bar{Y}_c^\alpha \quad (6)$$

Two types of local problems imposed in  $Y_m$  must be solved for characteristic displacements  $\omega^{ij}$  and  $\omega^p$  being  $Y$ -periodic functions from the Sobolev space  $H^1(Y^\alpha)$  consisting of functions with the first derivatives in  $L^2(Y^\alpha)$ ; this space is denoted by  $\mathbf{H}_\#^1(Y^\alpha)$ :

Find  $\omega^{ij} \in \mathbf{H}_\#^1(Y^\alpha)$  and  $\omega^p \in \mathbf{H}_\#^1(Y^\alpha)$  satisfying

$$a_y^m(\omega^{ij} + \mathbf{\Pi}^{ij}, \mathbf{v}) = 0, \quad i, j = 1, 2, 3, \quad (7)$$

$$a_y^m(\omega^p, \mathbf{v}) = \frac{1}{|Y^\alpha|} \int_{\Gamma_m} \mathbf{v} \cdot \mathbf{n}^m dS_y, \quad (8)$$

where  $\mathbf{\Pi}^{ij} = (\Pi_k^{ij})$ ,  $i, j, k = 1, 2, 3$  with  $\Pi_k^{ij} = y_j \delta_{ik}$  and  $a_y^m$  is the bilinear form defined as follows:

$$a_y^m(\mathbf{w}, \mathbf{v}) = \frac{1}{|Y^\alpha|} \int_{Y_m} (\mathbb{D} \nabla_y^S \mathbf{w}) : \nabla_y^S \mathbf{v}. \quad (9)$$

## 2.3 Model obtained by homogenization

The effective properties of the deformable porous medium are introduced using the characteristic responses obtained as the solutions of (12)

$$A_{ijkl} = a_y^m(\omega^{ij} + \mathbf{\Pi}^{ij}, \omega^{kl} + \mathbf{\Pi}^{kl}), \quad B_{ij} = -\frac{1}{|Y^\alpha|} \int_{Y_m} \text{div}_y \omega^{ij}, \quad M = a_y^m(\omega^p, \omega^p), \quad (10)$$

where both the tensors are symmetric, i.e.  $\mathbb{A} = (A_{ijkl})$  satisfies  $A_{ijkl} = A_{klij} = A_{jikl}$  and  $\mathbf{B} = (B_{ij})$  satisfies  $B_{ij} = B_{ji}$ . Obviously,  $M > 0$ .

At the first level of the homogenization process, we obtain the model of poroelasticity governing the skeleton displacement  $\mathbf{u} \in V(\Omega)$  and the fluid pressure  $\bar{p} \in \mathbb{R}$  which verify the following equations:

$$\int_{\Omega} (\mathbb{A} \nabla_x^S \mathbf{u} - \bar{p} \hat{\mathbf{B}}) : \nabla_x^S \mathbf{v} = \int_{\Omega} (1 - \phi) \mathbf{f} \cdot \mathbf{v} + \int_{\partial\Omega} \bar{\mathbf{g}} \cdot \mathbf{v} dS_x \quad \forall \mathbf{v} \in V(\Omega) \quad (11)$$

$$\int_{\Omega} \hat{\mathbf{B}} \nabla_x^S \mathbf{u} + \bar{p} (M + \bar{\phi} \gamma) |\Omega| = -J, \quad \hat{\mathbf{B}} := \mathbf{B} + \phi \mathbf{I} \quad (12)$$

where  $V(\Omega)$  is the space of kinematically admissible displacements (we omit details on various types of the boundary conditions and solvability conditions, see [3] for details),  $J$  is the limit of total fluid injection,  $\bar{\mathbf{g}}$  is the mean surface traction and  $\bar{\phi}$  is the mean porosity. All  $\mathbb{A}$ ,  $\mathbf{B}$ ,  $M$ ,  $\phi$  and  $J$  are associated with the upscaling from the  $\alpha$ -level to the  $\beta$ -level and will be further labeled by the superscript  $\alpha$ .

## 2.4 Homogenization of the $\beta$ -level

In an analogy to the previous level,  $\beta$ -level is split into a matrix and canal. Note that in our case, the "canal" is represented by ellipsoidal lacuna. The name "canal" remains just for preserving subscript  $c$ . In Rohan et.all (2012), [3] the description of this level is as follows: displacement  $\mathbf{u}^{\beta,\varepsilon}$  and pressure  $\bar{p}^\varepsilon$  must satisfy

$$\int_{\Omega_m^{\beta,\varepsilon}} (\mathbb{A}^\alpha \nabla^S \mathbf{u}^{\beta,\varepsilon} - \bar{p}^\varepsilon \hat{\mathbf{B}}^\alpha) : \nabla^S \mathbf{v} + \bar{p}^\varepsilon \int_{\Gamma^{\beta,\varepsilon}} \mathbf{v} \cdot \mathbf{n}^m dS_x = \int_{\partial\Omega_m^{\beta,\varepsilon}} \bar{\mathbf{g}}^\alpha \cdot \mathbf{v} dS_x + \int_{\Omega_m^{\beta,\varepsilon}} \hat{\mathbf{f}}^\alpha \cdot \mathbf{v}, \quad \forall \mathbf{v} \in V(\Omega_m^{\beta,\varepsilon}), \quad (13)$$

and

$$\int_{\Omega_m^{\beta,\varepsilon}} (\hat{\mathbf{B}}^\alpha : \nabla^S \mathbf{u}^{\beta,\varepsilon} + \int_{\partial\Omega_c^{\beta,\varepsilon}} \tilde{\mathbf{u}}^{\beta,\varepsilon} \cdot \mathbf{n}^c dS_x + \bar{p}^\varepsilon [(M^\alpha) + \gamma \bar{\phi}^\alpha |\Omega_m^{\beta,\varepsilon}| + \gamma |\Omega_c^{\beta,\varepsilon}|]) = -J^{\beta,\varepsilon} \quad (14)$$

## 2.5 Homogenized problem on $\beta$ -level

The heterogeneities at the mesoscopic *beta*-level are represented by the RPC with an analogous decomposition as introduced in (6). Local problems on the  $\beta$ -level are introduced, as follows: Find  $\omega^{ij} \in \mathbf{H}_\#^1(Y^\alpha)$  and  $\omega^p \in \mathbf{H}_\#^1(Y^\alpha)$  satisfying

$$\int_{Y_m^\beta} [\mathbb{A}^\alpha \nabla_y^S (\omega^{ij} + \mathbf{\Pi}^{ij})] : \nabla_y^S \mathbf{v} = 0 \quad (15)$$

$$\int_{Y_m^\beta} [\mathbb{A}^\alpha \nabla_y^S \omega^p] : \nabla_y^S \mathbf{v} = - \int_{Y_m^\beta} \hat{\mathbf{B}}^\alpha : \nabla_y^S \mathbf{v} + \int_{\Gamma_V^\beta} \mathbf{v} \cdot \mathbf{n}^m dS_y \quad (16)$$

The effective poroelasticity properties are given by the following coefficients:

$$A_{ijkl}^\beta = \int_{Y_m^\beta} [\mathbb{A}^\alpha \nabla_y^S (\omega^{kl} + \mathbf{\Pi}^{kl})] : \nabla_y^S \mathbf{v} (\omega^{ij} + \mathbf{\Pi}^{ij}) \quad (17)$$

$$B_{ij}^\beta = \int_{Y_m^\beta} \hat{\mathbf{B}}^\alpha : \nabla_y^S \mathbf{v} (\omega^{ij} + \mathbf{\Pi}^{ij}) - \frac{1}{|Y_m^\beta|} \int_{Y_m^\beta} \text{div}_y \omega^{ij} \quad (18)$$

$$M^\beta = \int_{Y_m^\beta} [\mathbb{A}^\alpha \nabla_y^S (\omega^p)] : \nabla_y^S \mathbf{v} (\omega^p) \quad (19)$$

The response of the homogenized medium at macroscopic scale is described by the displacement  $\mathbf{u}$  and by pressure  $\bar{p}$  satisfying

$$\int_{\Omega^\beta} (\mathbb{A}^\beta \nabla_x^S \mathbf{u} - \bar{p} \hat{\mathbf{B}}^\beta) : \nabla_x^S \mathbf{v} = \int_{\Omega^\beta} (1 - \phi^\beta) \mathbf{f}^\alpha \cdot \mathbf{v} + \int_{\partial\Omega^\beta} \bar{\mathbf{g}}^\beta \cdot \mathbf{v} dS_x \quad \forall V(\Omega) \quad (20)$$

$$\int_{\Omega^\beta} \hat{\mathbf{B}}^\beta \nabla_x^S \mathbf{u} + \bar{p} \hat{M}^\beta |\Omega^\beta| = -J^\beta, \quad (21)$$

where

$$\hat{\mathbf{B}}^\beta := \mathbf{B}^\beta + \phi^\beta \mathbf{I}, \quad \hat{M}^\beta := M^\beta + \gamma \bar{\phi}^\beta + (M^\alpha + \gamma \bar{\phi}^\alpha)(1 - \bar{\phi}^\beta). \quad (22)$$

## 3 Geometry

In this section, the geometry, which was used as the representation of the  $\alpha$ -level and  $\beta$ -level structure, is presented. For both geometry creation and meshing was used the software *GMSH*. In the case of our model, when the periodic structure is considered, the generated mesh must be also periodic.

### 3.1 Geometry on $\alpha$ -level

A cubic cell  $Y^\alpha$  with a characteristic length  $L$  was used. Note, that numbers of canaliculi differ in X, Y, Z direction. To determine the number of canaliculi in each direction, we followed the approach from [1]. Using the number of canaliculi per lacuna  $N.Ca$ , projected surface areas for the osteocyte lacunar ellipsoid in the X-Z, X-Y and Y-Z planes  $PSA_{xz}$ ,  $PSA_{xy}$ ,  $PSA_{yz}$  and their sum  $T_{PSA}$ , we can determine number of canaliculi in X, Y and Z direction  $n_x, n_y, n_z$ . On the alpha level we have to calculate the

number of canaliculi in each direction from Eq.(23).

$$n_i = \frac{PSA_{jk}}{2T_{PSA}} N.Ca, \quad i, j, k = x, y, z. \quad (23)$$

From the Eq.(23) it is clear, that the size of lacunae determined by semi-axes  $a_0, b_0, c_0$  allows for determination of the number of canaliculi in each direction. The numerous canaliculi are approximated by one bigger canal in each direction with a corresponding diameter. This simplification is reasonable - the modelling of numerous small canals would consume a lot of computational time and we expect only small impact on result. The resulting mesh can be seen on Fig.1.

### 3.2 Geometry on $\beta$ -level

The  $\beta$ -level geometry represents lacunae in a matrix characterized by elastic properties obtained by homogenization on the previous level. We created a cubic periodic cell with characteristic length  $L$ . The lacunae is represented by an ellipsoid defined by semi-axes  $a_0, b_0, c_0$ , which determine the size of lacunae. The resulting mesh can be seen on Fig.1.

Symbol	Parameter	Unit	$\alpha$ -level	$\beta$ -level
$E$	Young's modulus	GPa	18.0	-
$\nu$	Poisson's ration	-	0.3	-
$\gamma$	fluid compressibility	GPa <sup>-1</sup>	0.9	-
$L$	characteristic length of RPC	$\mu m$	4.3	43
$r_x$	diameter of canaliculi in x-direction	$\mu m$	0.6-1.8	-
$r_y$	diameter of canaliculi in y-direction	$\mu m$	0.6	-
$r_z$	diameter of canaliculi in z-direction	$\mu m$	0.6	-
$a_0$	semi-axis of ellipsoid in x-direction	$\mu m$	-	2.5
$b_0$	semi-axis of ellipsoid in y-direction	$\mu m$	-	12.5
$c_0$	semi-axis of ellipsoid in z-direction	$\mu m$	-	5.0
$N.Ca$	number of canaliculi per lacunae	-	106	-

**Tab. 1** Input parameters of model for  $\alpha$ -level and  $\beta$ -level

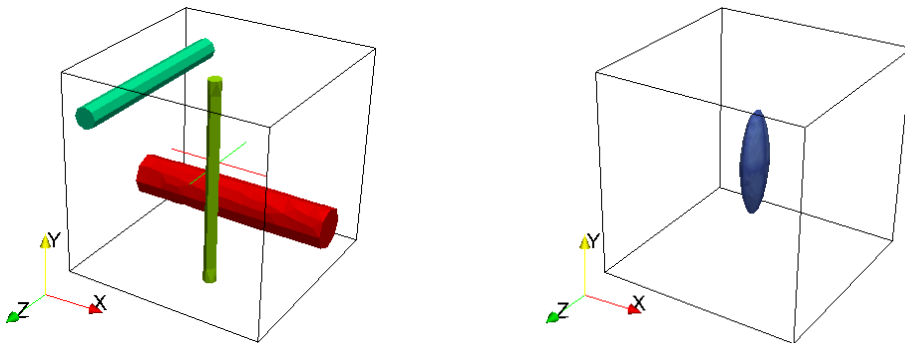


**Fig. 1** Left – geometry on  $\alpha$ -level; Right – geometry on  $\beta$ -level

## 4 Parameter study

The mathematical model from the section above was implemented in SfePy, software for solving systems of coupled partial differential equations by the finite element method, see <http://sfepy.org>.

All of the used input arguments, namely the material properties on microscopic level and the geometric properties of the mesh are shown in Tab.1.

A parameter study was performed; the porosity on  $\alpha$ -level was changed by increasing the  $x$ -direction canaliculi diameter  $r_x$ . The  $y$ -direction and  $z$ -direction was kept constant. The structure on  $\alpha$ -level was oriented in  $x$ -axis direction. Logically, this caused a change of the poroelastic properties on the macroscopic level. The dependency of Young's modulus and Poisson's ratio on  $\phi_\gamma$  porosity, where  $\phi_\gamma = \phi_\alpha + \phi_\beta - \phi_\alpha\phi_\beta$ , is shown in the Fig.2. It can be seen that using the isotropic material considered at the microscopic level we an orthotropic material has been obtained on the macroscopic level, whose anisotropy increases with the change of porosity.

## 5 CONCLUSIONS

The presented homogenized model can be used for modelling cortical bone tissue. Various geometries representing fluid saturated porous structure related to microscopic and mesoscopic level were considered. The influence of changing one of the  $\alpha$ -level geometric parameters on the homogenized coefficients, related to macroscopic level, was studied. This modelling approach is proposed as an advanced hierarchical description of poroelastic properties of the cortical bone tissue, but a wide range of further applications is expected.

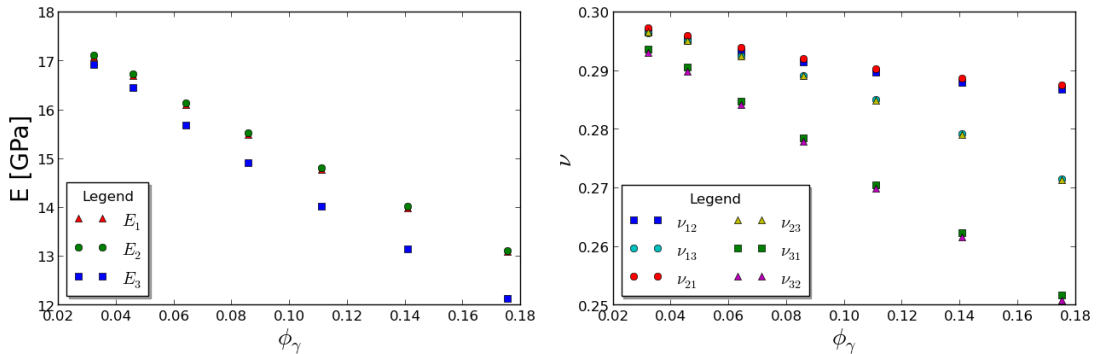


**Fig. 2** The dependency of poroelastic properties on porosity change caused by increase of  $r_x$ : Left – Young's modulus; Right – Poisson's ratio

## ACKNOWLEDGEMENT

The work has been elaborated with the support of project SGS-2013-026 and in part by the project IGA, NT-13326.

## REFERENCES

- [1] Beno, T., & al.: Estimation of Bone Permeability Using Accurate Microstructural Measurements. *Journal of Biomechanics*.2006,XXXIX, pp. 2378-2387. ISSN: 0021-9290.
- [2] HELLMICH, C. & al. Mineral-collagen Interactions in Elasticity of Bone Ultrastructure - a Continuum Micromechanics Approach. *European Journal of Mechanics and Solids*. 2004, XXIII, Nr. 5, pp. 783-810. ISSN: 0997-7538.
- [3] ROHAN, E. & at al. Hierarchical Homogenization of Fluid Saturated Porous Solid with Multiple Porosity Scales. *C. R. Mecanique*. 2012, CCCXL, Nr. 10, pp. 688-694. ISSN: 1631-0721.
- [4] YOON, Y.J. & COWIN, S. C. An Estimate of Anisotropic Poroelastic Constants of an Osteon. *Biomechan Model Mechanobiol*. 2008, VII, Nr. 1, pp. 13-26. ISSN: 1617-7959.